GEOPHYSICS, VOL. 61, NO. 2 (MARCH-APRIL 1996); P. 467–483, 10 FIGS.

P-wave signatures and notation for transversely isotropic media: An overview

Ilya Tsvankin*

ABSTRACT

Progress in seismic inversion and processing in anisotropic media depends on our ability to relate different seismic signatures to the anisotropic parameters. While the conventional notation (stiffness coefficients) is suitable for forward modeling, it is inconvenient in developing analytic insight into the influence of anisotropy on wave propagation. Here, a consistent description of *P*-wave signatures in transversely isotropic (TI) media with arbitrary strength of the anisotropy is given in terms of Thomsen notation.

The influence of transverse isotropy on *P*-wave propagation is shown to be practically independent of the vertical *S*-wave velocity V_{S0}, even in models with strong velocity variations. Therefore, the contribution of transverse isotropy to *P*-wave kinematic and dynamic signatures is controlled by just two anisotropic parameters, ε and δ, with the vertical velocity V_{P0} being a scaling coefficient in homogeneous models.

The distortions of reflection moveouts and amplitudes are not necessarily correlated with the magnitude of velocity anisotropy. The influence of transverse isotropy on *P*-wave normal-moveout (NMO) velocity in a horizontally layered medium, on small-angle reflection coefficient, and on point-force radiation in the symmetry direction is entirely determined by the parameter δ. Another group of signatures of interest in reflection seismology—the dip-dependence of NMO velocity, magnitude of nonhyperbolic moveout, time-migration impulse response, and the radiation pattern near vertical—is dependent on both anisotropic parameters (ε and δ) and is primarily governed by the difference between ε and δ. Since *P*-wave signatures are so sensitive to the value of $\varepsilon - \delta$, application of the elliptical-anisotropy approximation ($\varepsilon = \delta$) in *P*-wave processing may lead to significant errors.

Many analytic expressions given in the paper remain valid in transversely isotropic media with a tilted symmetry axis. Moreover, the equation for NMO velocity from dipping reflectors, as well as the nonhyperbolic moveout equation, can be used in symmetry planes of any anisotropic media (e.g., orthorhombic).

INTRODUCTION: CONVENTIONAL AND THOMSEN NOTATION

The influence of anisotropy on seismic processing and interpretation is well documented in the literature (e.g., Banik, 1984; Winterstein, 1986; Sams et al., 1993; Larner, 1993). However, the large number of independent parameters required to describe anisotropic models makes seismic inversion and processing in anisotropic media difficult. Further progress in extending seismic algorithms to anisotropic media requires a better understanding of the dependence of seismic signatures on the parameters of the anisotropic velocity field. In spite of significant attention devoted to this problem, there is no consistent description of body-wave velocities and amplitudes in transversely isotropic (TI) media. One of the main reasons for this situation is that the notations used by different authors are incompatible with each other and often are not convenient in describing seismic wave propagation.

Although the matter of notation seems trivial, it is of utmost importance in studying seismic signatures in anisotropic media. Historically, wave propagation was described using the elastic (stiffness) coefficients c_{ij}. Since both Hooke's law and the wave equation are expressed through the stiffnesses c_{ij}, these coefficients are convenient to use in all types of forward-modeling algorithms. The problems arise when it is necessary to go beyond specific examples and find the effective parameters that govern seismic wavefields in anisotropic media. As shown by the discussion of various *P*-wave signatures below, the conventional notation is not well-suited for this purpose. Without an

Manuscript received by the Editor July 22, 1994; revised manuscript received May 1, 1995.
*Center for Wave Phenomena, Colorado School of Mines, Golden, CO 80401-1887.

understanding of the relations between the medium parameters and seismic signatures, it is hardly possible to make qualitative estimates of the influence of anisotropy on seismic wavefields and, even more importantly, to develop inversion and processing algorithms for anisotropic media.

Throughout the paper, I assume that the medium is transversely isotropic with a vertical symmetry axis, or VTI. (The expressions for an unbounded homogeneous medium are valid for any orientation of the symmetry axis.) The main disadvantages of the conventional notation in VTI media can be summarized as follows:

1) The strength of the anisotropy is hidden in the elastic coefficients. The medium is isotropic if $c_{11} = c_{33}$, $c_{44} = c_{66}$, and $c_{13} = c_{33} - 2c_{44}$; clearly, it is difficult to estimate the degree of velocity anisotropy just from inspection of the elastic constants. Also, the condition satisfied by elliptically anisotropic media is complicated.
2) Since most reflection data are acquired at small offsets, it would be useful to have a parameter responsible for *P*-wave velocity near the (vertical) symmetry axis. However, no such parameter exists in the conventional notation.
3) *P-SV* propagation is described by four stiffness coefficients: c_{11}, c_{33}, c_{44}, and c_{13}. As I show below, by using Thomsen notation it is possible to reduce the number of independent parameters needed to describe *P*-wave signatures. Also, the inversion of *P*-wave traveltime data for the c_{ij} coefficients is ambiguous because the trade-off between c_{44} and c_{13} cannot be resolved from *P*-wave data alone; this will be discussed in the section about *P*-wave phase and group velocity.
4) The expressions for normal-moveout velocities in the conventional notation are complicated. Since surface seismic processing operates with reflection moveouts, it is important to have easily tractable equations for NMO velocities in anisotropic media.

An improvement over the conventional notation can be achieved by targeting the combinations of elastic constants most suitable for the description of seismic wavefields. An alternative notation based on this principle was suggested by Thomsen (1986). The idea of the Thomsen parameters is to separate the influence of the anisotropy from the "isotropic" quantities, i.e., *P* and *S* velocities along the symmetry axis (I omit the qualifiers in "quasi-*P*-wave" and "quasi-*SV*-wave"). Five independent elastic coefficients needed to describe vertical transverse isotropy (c_{11}, c_{33}, c_{44}, c_{66}, and c_{13}) can be replaced by the vertical velocities V_{P0} and V_{S0} of *P*- and *S*-waves, respectively, and three dimensionless anisotropic parameters ε, δ, and γ (Thomsen, 1986):

$$V_{P0} \equiv \sqrt{\frac{c_{33}}{\rho}}, \tag{1}$$

$$V_{S0} \equiv \sqrt{\frac{c_{44}}{\rho}}, \tag{2}$$

$$\varepsilon \equiv \frac{c_{11} - c_{33}}{2c_{33}}, \tag{3}$$

$$\delta \equiv \frac{(c_{13} + c_{44})^2 - (c_{33} - c_{44})^2}{2c_{33}(c_{33} - c_{44})}, \tag{4}$$

$$\gamma \equiv \frac{c_{66} - c_{44}}{2c_{44}}, \tag{5}$$

where ρ is the density.

P- and *SV*-wave signatures depend on four coefficients – V_{P0}, V_{S0}, ε, and δ, while the *SH*-wave is fully described by the vertical velocity V_{S0} and parameter γ.

One subtle point in the relation between the conventional notation and Thomsen parameters needs to be mentioned. From equations (1) through (5) it is clear that V_{P0}, V_{S0}, ε, δ, and γ are uniquely defined by the stiffness coefficients. The inverse transition from Thomsen parameters to the stiffnesses, however, is unique for only four coefficients (c_{11}, c_{33}, c_{44}, and c_{66}). The fifth coefficient, c_{13}, can be uniquely determined from equation (4) only if the sign of the sum $c_{13} + c_{44}$ is specified. In principle, it is possible for the coefficient c_{13}, as well as for the sum $c_{13} + c_{44}$, to be negative (Helbig and Schoenberg, 1987). Helbig and Schoenberg (1987) also show that while phase velocities are not dependent on the sign of $c_{13} + c_{44}$, *P*-wave polarizations in media with $c_{13} + c_{44} < 0$ become anomalous (e.g., the polarization vector may even become perpendicular to the phase-velocity vector). However, since models with negative $c_{13} + c_{44}$ are extremely rare (in this case, c_{13} should be negative and relatively large), for practical purposes of seismic modeling and processing it can be assumed that $c_{13} + c_{44} > 0$. Note that if δ is small (a common case), it can be approximated by $\delta \approx (c_{13} + 2c_{44} - c_{33})/c_{33}$ (Thomsen, 1993), and the problem with the unique determination of c_{13} does not arise.

Some of the advantages of Thomsen notation are immediately obvious. The dimensionless anisotropies ε, δ, and γ go to zero for isotropic media and, therefore, conveniently characterize the strength of the anisotropy. The parameter ε, close to the fractional difference between the horizontal and vertical *P*-wave velocities, defines what is often simplistically called the "*P*-wave anisotropy." Likewise, γ represents the same measure for *SH*-waves. The parameter δ is responsible for near-vertical *P*-wave velocity variations; as shown in Thomsen (1986), it is δ rather than ε that determines the influence of anisotropy on short-spread reflection data. It should be mentioned, however, that the Thomsen parameters are less convenient for describing seismic signatures that depend on near-horizontal velocity variations; this situation is typical for crosswell geometries in VTI media.

Another advantage of Thomsen notation is the simplicity of the elliptical condition: ε = δ in elliptically anisotropic media. In this case, the *P*-wave slowness surface and the wavefront are elliptical, while the *SV*-wave velocity is independent of angle, implying a spherical wavefront. For *SH*-waves, transverse isotropy always means elliptical anisotropy, with the degree of the velocity variations determined by the parameter γ. At the same time, for *P* and *SV*-waves, elliptical anisotropy is just a special case of transverse isotropy. As we will see throughout the paper, the sensitivity of *P*-wave signatures to deviations from elliptical anisotropy makes the difference ε − δ one of the most important parameters in surface seismic processing.

Existing laboratory and field data indicate that the horizontal velocity of *P*- and *SH*-waves is usually larger than the vertical velocity, i.e., that the parameters ε and γ are predominantly positive (Thomsen, 1986). Also, most measurements made for transversely isotropic formations at seismic frequencies indicate that $\varepsilon > \delta$ (Thomsen, 1986; Sayers, 1994; Tsvankin and Thomsen, 1994). For instance, $\varepsilon > \delta$ for transversely isotropic media caused by the thin bedding of isotropic layers (Berryman, 1979).

The introduction of the dimensionless anisotropic coefficients allowed Thomsen (1986) to develop the weak-anisotropy approximation ($|\varepsilon| \ll 1$, $|\delta| \ll 1$, $|\gamma| \ll 1$) by linearizing seismic velocities, and group and polarization angles in ε, δ, and γ. The weak-anisotropy approximation is an extremely powerful tool in understanding the behavior of seismic wavefields in anisotropic media. At the same time, it should not be regarded as a substitute for the exact equations in modeling, inversion, and processing algorithms. Below, I use the weak-anisotropy approximation to gain analytic insight into different wave-propagation problems.

Although originally designed for weakly anisotropic models, the dimensionless anisotropic parameters turned out to be convenient in TI media with arbitrary strength of velocity anisotropy. This point, which is not well understood in the literature, will be repeatedly stressed throughout the paper.

The following sections are devoted to a systematic description of body-wave velocities, polarizations, and amplitudes in transversely isotropic media. The present discussion is focused on *P*-waves, which represent a majority of data being acquired in oil and gas exploration. However, most of the analytic developments discussed here can be easily applied to *SV*-waves as well. Treatment of *SH*-waves in transversely isotropic media is straightforward because *SH*-wave anisotropy is elliptical.

KINEMATIC PROPERTIES

Phase and group velocity

Here, I present two refinements to the phase-velocity equations given in Thomsen (1986). First, the *exact* phase velocity for *P*- and *SV*-waves is expressed in a relatively simple fashion through the anisotropies ε and δ. Second, the phase-velocity term quadratic in ε and δ is derived and used to estimate the influence of V_{S0} on the *P*-wave phase velocity. The results in this section are given for an unbounded homogeneous medium and can be used for any orientation of the symmetry axis.

The formula for the *P*-wave phase velocity in standard notation can be found, for instance, in White (1983):

$$2\rho V^2(\theta) = (c_{11} + c_{44}) \sin^2\theta + (c_{33} + c_{44}) \cos^2\theta + \{[(c_{11} - c_{44}) \sin^2\theta - (c_{33} - c_{44}) \cos^2\theta]^2 + 4(c_{13} + c_{44})^2 \sin^2\theta \cos^2\theta\}^{1/2}, \tag{6}$$

where θ is the phase angle measured from the symmetry axis. To obtain the *SV*-wave velocity, the plus sign in front of the radical should be replaced with a minus.

Dividing both parts of equation (6) by the squared vertical velocity V_{P0}^2 [equation (1)] and substituting the anisotropic coefficients ε [equation (3)] and δ [equation (4)] yields the exact phase-velocity function expressed through the Thomsen parameters:

$$\frac{V^2(\theta)}{V_{P0}^2} = 1 + \varepsilon \sin^2\theta - \frac{f}{2} + \frac{f}{2}\sqrt{1 + \frac{4\sin^2\theta}{f}(2\delta\cos^2\theta - \varepsilon\cos 2\theta) + \frac{4\varepsilon^2\sin^4\theta}{f^2}}, \tag{7}$$

where

$$f \equiv 1 - V_{S0}^2/V_{P0}^2 = 1 - c_{44}/c_{33} \tag{8}$$

is the only term containing the *S*-wave vertical velocity. This is equivalent to equations (10a) and (10b) from Thomsen (1986); however, the velocity equations in Thomsen's paper are more complicated and contain an intermediate coefficient δ^* instead of δ.

For elliptical anisotropy ($\varepsilon = \delta$), the *P*-wave phase velocity becomes (exactly)

$$\frac{V^2(\theta)}{V_{P0}^2} = 1 + 2\delta\sin^2\theta = 1 + 2\varepsilon\sin^2\theta. \tag{9}$$

Equation (7) can be simplified further by separating out under the radical a "nonelliptical" term containing $\varepsilon - \delta$:

$$\frac{V^2(\theta)}{V_{P0}^2} = 1 + \varepsilon\sin^2\theta - \frac{f}{2} + \frac{f}{2}\sqrt{\left(1 + \frac{2\varepsilon\sin^2\theta}{f}\right)^2 - \frac{2(\varepsilon - \delta)\sin^2 2\theta}{f}}. \tag{10}$$

As before, the squared *SV*-wave velocity (normalized by V_{P0}^2) can be obtained by putting a minus sign before the radical. From comparison of equation (10) with equation (6) it is clear that the exact phase velocity, both for *P*- and *SV*-waves, becomes no more complicated when represented as a function of ε and δ.

Let us now transform the phase-velocity equation (10) under the assumption of weak anisotropy ($|\varepsilon| \ll 1$, $|\delta| \ll 1$). Expanding the radical in a Taylor series and dropping terms quadratic in the anisotropies ε and δ, we obtain

$$\frac{V^2(\theta)}{V_{P0}^2} = 1 + 2\delta\sin^2\theta\cos^2\theta + 2\varepsilon\sin^4\theta, \tag{11}$$

or, separating the elliptical and nonelliptical terms,

$$\frac{V^2(\theta)}{V_{P0}^2} = 1 + 2\delta\sin^2\theta + 2(\varepsilon - \delta)\sin^4\theta. \tag{12}$$

Taking the square root and linearizing equation (11) further in ε and δ leads to Thomsen's (1986) weak-anisotropy approximation

$$V(\theta) = V_{P0}(1 + \delta\sin^2\theta\cos^2\theta + \varepsilon\sin^4\theta). \tag{13}$$

The *P*-wave phase velocity, linearized in ε and δ [equation (13)], is independent of the shear-wave vertical velocity V_{S0}. To estimate the contribution of V_{S0}, the weak-anisotropy approximation can be refined by adding terms that are quadratic in the anisotropies.

Note that for elliptical anisotropy the weak-anisotropy formula for the squared velocity (12) reduces to the exact expression (9). Hence, our refinement to the weak-anisotropy approximation for the squared velocity should contain the difference $\varepsilon - \delta$. Therefore, equation (10), which contains an explicitly separated nonelliptical term, is ideally suited for our purposes. By expanding the radical in equation (10) in a Taylor series and retaining the terms quadratic in ε and δ, we find

$$\frac{V^2(\theta)}{V_{P0}^2} = 1 + 2\delta \sin^2\theta \cos^2\theta + 2\varepsilon \sin^4\theta + \frac{4}{f}(\varepsilon - \delta)(\varepsilon \sin^2\theta + \delta\cos^2\theta)\sin^4\theta\cos^2\theta. \qquad (14)$$

Equation (14) can be called the "moderate-anisotropy approximation" for the squared P-wave phase velocity since it contains the terms linear and quadratic in the anisotropies ε and δ. As expected, the quadratic term vanishes for elliptical anisotropy. However, if we continued the derivation to find a similar expansion for the phase velocity itself, it would contain a quadratic term that does not go to zero for $\varepsilon = \delta$; this is clear from the fact that equation (13) is not exact for elliptical anisotropy.

Because of these quadratic terms, equation (14) is numerically more accurate than equation (11), and may be used with larger ε and δ. However, formula (14) serves best in developing analytic insight into the influence of the shear-wave vertical velocity V_{S0} on P-wave phase velocity. The contribution of V_{S0} [or f; see equation (8)] is limited to the quadratic term in equation (14). For a practically important range of V_{S0} corresponding to $2.5 > V_{P0}/V_{S0} > 1.5$, f changes from 1.19 to 1.8; hence f and the quadratic term as a whole change by about 50%. This is a substantial variation that can lead to tangible phase-velocity changes provided the quadratic term itself is significant. However, the quadratic term vanishes for $\theta = 0°$ and $\theta = 90°$, and remains relatively small at intermediate angles. Of course, this conclusion applies to the range of ε and δ for which equation (14) can be used. For instance, for a model with $\varepsilon = 0.5$, and $\delta = 0$, formula (14) predicts just a 1.8% maximum variation in the P-wave phase velocity over the range in V_{P0}/V_{S0} from 1.5 to 2.5. Moreover, the estimates of the influence of V_{S0} based on equation (14) turn out to be overstated because the contribution of the neglected higher-order terms reduces the influence of V_{S0} even further. For the same model with $\varepsilon = 0.5$, and $\delta = 0$, the exact phase velocity changes by no more than 0.6% for the range of the shear-wave vertical velocity considered above.

Figure 1 shows the influence of V_{S0} on the exact P-wave phase velocity for several combinations of ε and δ. With increasing difference $\varepsilon - \delta$, the curves corresponding to two extreme values of V_{S0} diverge slightly from each other, but the overall contribution of the variations in the S-wave vertical velocity remains practically negligible, even for uncommonly strong velocity anisotropy. Comparison of the two media with $\varepsilon = 0.8$ in Figure 1 demonstrates that the magnitude of the influence of V_{S0} is controlled more by the difference between ε and δ than by the individual values of the coefficients: the dependence of the P-wave phase velocity on V_{S0} is less pronounced for the model with larger δ but smaller $\varepsilon - \delta$.

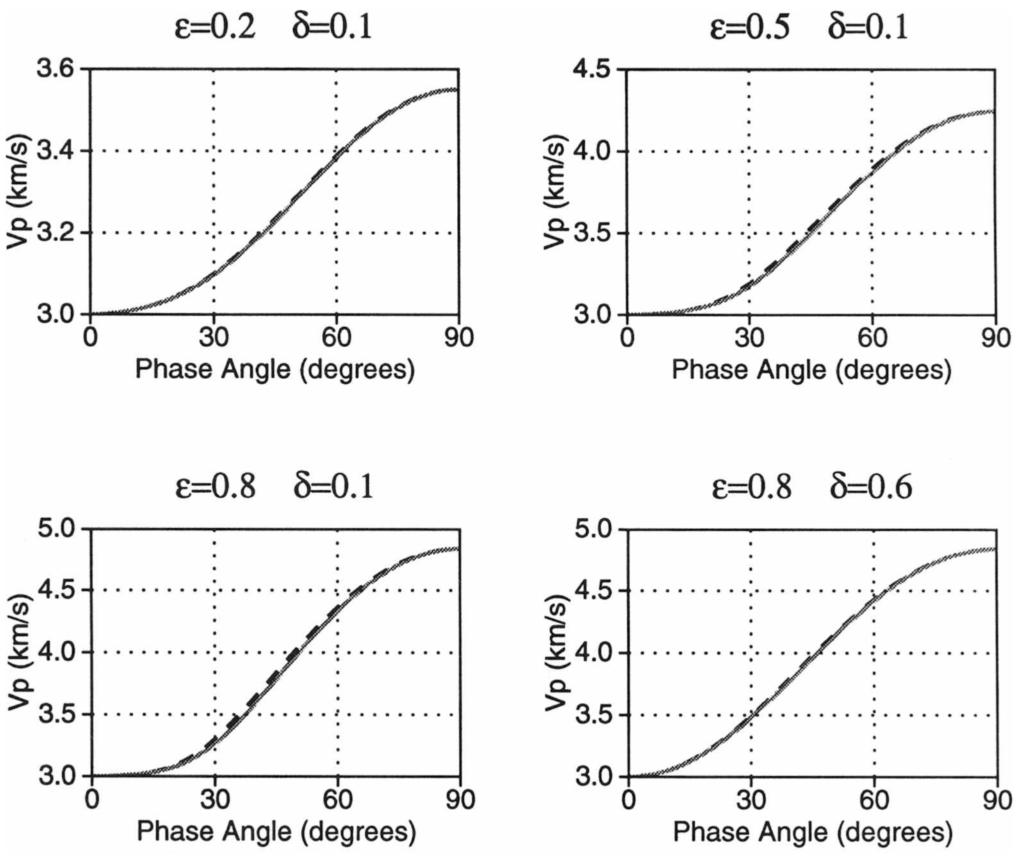

FIG. 1. P-wave phase velocity for two V_{P0}/V_{S0} ratios. The dashed curve corresponds to $V_{P0}/V_{S0} = 1.5$, the solid gray curve to $V_{P0}/V_{S0} = 2.5$.

It is intuitively comfortable to reach this conclusion of the negligibility of V_{S0} in the expression for P-wave phase velocity. However, since V_{S0} appears several times in equation (7), this analytic and numerical verification of intuition is useful. It should be emphasized that in the conventional notation, the influence of $c_{44} = \rho V_{S0}^2$ on P-wave velocity cannot be ignored. We have been able to reduce the number of parameters by switching to Thomsen notation, because the influence of c_{44} is absorbed by the parameter δ [equation (4)].

Phase velocity is a fundamentally important function in anisotropic wave propagation because it determines (along with its derivatives) the expressions for group and moveout velocities, as well as the group (ray) angles. In general, any kinematic P-wave signature in transversely isotropic media can be represented as

$$K_P \approx K_P^{isot} + L(\varepsilon, \delta) + Q(\varepsilon, \delta, V_{S0}), \qquad (15)$$

where K_P^{isot} is the isotropic signature ($\varepsilon = 0, \delta = 0$), L is the term linear in the anisotropies ε and δ, and Q denotes the quadratic and other higher-order terms in ε and δ, which contain V_{S0}. Since the S-wave vertical velocity V_{S0} contributes only to the second correction term Q, its influence is not significant unless, in some particular case, the anisotropic terms dominate the function K_P (one such case is described in the section about normal-moveout velocity). The weak dependence of the P-wave phase velocity on the S-wave vertical velocity implies that the influence of V_{S0} can be expected to be small in all kinematic problems involving P-waves.

The group velocity responsible for energy propagation is expressed (exactly) through phase velocity as (Berryman, 1979)

$$v_{gr} = V\sqrt{1 + \left(\frac{1}{V}\frac{dV}{d\theta}\right)^2}, \qquad (16)$$

and the derivative $dV/d\theta$, linearized in ε and δ, is given by

$$\frac{dV_P(\theta)}{d\theta} = V_{P0} \sin 2\theta\,(\delta \cos 2\theta + 2\varepsilon \sin^2\theta). \qquad (17)$$

Since the term containing the first derivative of phase velocity is squared, it has only quadratic and higher-order terms in ε and δ. Therefore, in the weak-anisotropy approximation, linearized in ε and δ, the group velocity as a function of the phase angle coincides with the phase velocity. However, the group velocity should be evaluated not at the phase angle, but instead at the group angle ψ expressed through the phase angle as (Berryman, 1979)

$$\tan\psi = \frac{\tan\theta + \dfrac{1}{V}\dfrac{dV}{d\theta}}{1 - \dfrac{\tan\theta}{V}\dfrac{dV}{d\theta}} = \tan\theta\left[1 + \frac{\dfrac{1}{V}\dfrac{dV}{d\theta}}{\sin\theta\cos\theta\left(1 - \dfrac{\tan\theta}{V}\dfrac{dV}{d\theta}\right)}\right]. \qquad (18)$$

Dropping the terms quadratic in ε and δ from equation (18) yields for P-waves (Thomsen, 1986)

$$\tan\psi = \tan\theta[1 + 2\delta + 4(\varepsilon - \delta)\sin^2\theta]. \qquad (19)$$

Because of the presence of terms linear in the anisotropies in equation (19), the difference between the group and phase *angles* is more pronounced than that between the phase and group *velocities*. Also note that in the symmetry direction and in the isotropy plane, the phase and group velocities and angles coincide with each other. The conclusion about the weak influence of the S-wave vertical velocity drawn for the phase-velocity function, holds for the P-wave group velocity as well.

In reflection seismology, we are interested not just in the group velocity itself, but rather in the behavior of reflection moveout, which depends on the group velocity and group angle. Normal-moveout velocity and nonhyperbolic reflection moveout are examined in the following sections.

Normal-moveout velocity for horizontal reflectors

Anisotropy causes two major distortions of reflection moveouts. First, the normal (short-spread) moveout velocity is not equal to the root-mean-square (rms) vertical velocity (e.g., Banik, 1984). Second, anisotropy may enhance deviations from hyperbolic moveout since reflection moveout is generally nonhyperbolic even in a single homogeneous anisotropic layer (Hake et al., 1984).

Reflection moveout is usually approximated by the Taylor series expansion near vertical (Taner and Koehler, 1969):

$$t_T^2 = A_0 + A_2 x^2 + A_4 x^4 + \cdots, \qquad (20)$$

with the coefficients

$$A_0 = t_0^2, \qquad A_2 = \left.\frac{d(t^2)}{d(x^2)}\right|_{x=0}, \qquad A_4 = \frac{1}{2}\frac{d}{d(x^2)}\left[\frac{d(t^2)}{d(x^2)}\right]\Bigg|_{x=0}, \qquad (21)$$

where t_0 is the two-way vertical arrival time.

The quantity of most practical importance in exploration is the normal-moveout velocity V_{nmo}, which determines the hyperbolic moveout on conventional-length spreads comparable to the distance between the common midpoint (CMP) and the reflector.

$$V_{\text{nmo}}^2 = 1/A_2 = \left.\frac{d(x^2)}{d(t^2)}\right|_{x=0}. \qquad (22)$$

In a horizontally layered, transversely isotropic model with a vertical axis of symmetry, the normal-moveout velocity is equal to the rms average of the NMO velocities in the individual layers (Hake et al., 1984):

$$V_{\text{nmo}}^2 = \frac{1}{t_0}\sum_{i=1}^{N}[V_{\text{nmo}}^{(i)}]^2 \Delta t_0^{(i)}, \qquad (23)$$

where $V_{\text{nmo}}^{(i)}$ and $\Delta t_0^{(i)}$ are the NMO velocity and vertical traveltime in layer i.

The values of normal-moveout velocities in a single layer for different wave types can be expressed through the anisotropic coefficients as follows (Thomsen, 1986):

$$V_{\text{nmo}}^2[P\text{-wave}] = V_{P0}^2(1 + 2\delta), \qquad (24)$$

$$V_{\text{nmo}}^2[SV\text{-wave}] = V_{S0}^2(1 + 2\sigma), \qquad (25)$$

$$V_{\text{nmo}}^2[SH\text{-wave}] = V_{S0}^2(1 + 2\gamma), \qquad (26)$$

with

$$\sigma \equiv \left(\frac{V_{P0}}{V_{S0}}\right)^2 (\varepsilon - \delta). \tag{27}$$

It should be emphasized that these equations are valid for arbitrary strength of the anisotropy. The effective coefficient σ was introduced in Tsvankin and Thomsen (1994) as the most influential parameter in the SV-wave moveout and velocity equations. Here, I distinguish between the original Thomsen coefficients and their combinations, which are convenient to use in different applications; the latter will be called "effective" parameters. Note that the parameter σ goes to zero not only for isotropy, but also for elliptical anisotropy ($\varepsilon = \delta$).

Another "anellipticity" parameter (ε_s) was introduced in Carrion et al. (1992):

$$\varepsilon_s \equiv \frac{(c_{11} - c_{44})(c_{33} - c_{44}) - (c_{13} + c_{44})^2}{(c_{11} - c_{44})(c_{33} - c_{44})}. \tag{28}$$

The parameter ε_s governs the deviation of the P-wave slowness surface from elliptical and of the SV-wave slowness surface from circular. It is normalized so that $|\varepsilon_s| \le 1$; note that, unlike σ, ε_s is not designed to simplify the NMO velocity for the SV-wave.

In this paper, we are concerned mostly with P-wave signatures. Using equation (24), formula (23) can be rewritten for the P-wave as

$$V_{\text{nmo}}^2 = V_{\text{rms}}^2(1 + 2\xi), \tag{29}$$

where V_{rms} is the root-mean-square average of the true vertical velocities $V_{P0}^{(i)}$, and ξ is the value of δ averaged as follows over the stack of layers:

$$\xi = \frac{1}{V_{\text{rms}}^2 t_0} \sum_{i=1}^{N} [V_{P0}^{(i)}]^2 \, \delta^{(i)} \Delta t_0^{(i)}.$$

Equation (29) reduces to the conventional Dix (1955) formula only if the medium is isotropic or in the unlikely situation that the average value of δ is zero. Hence, if we try to derive interval vertical velocities $V_{P0}^{(i)}$ from equation (29) by applying the Dix formula, we get instead the NMO layer velocities, which contain a contribution of the anisotropic parameter δ. Ignoring the influence of δ in conventional processing leads to errors in time-to-depth conversion (e.g., Banik, 1984).

Hence, application of the anisotropic coefficients ε, δ, and γ makes it possible to obtain concise expressions for normal-moveout velocities that are valid for arbitrary strength of the anisotropy and are symmetric for all wave types. For the P-wave, the NMO velocity depends on the vertical velocity and the parameter δ responsible for near-vertical velocity variations.

Dip-dependence of NMO velocity

Reflection moveout from dipping interfaces is important both in the inversion of reflection data and in the development of dip-moveout (DMO) algorithms for anisotropic media. Conventional constant-velocity DMO is usually based on the cosine-of-dip correction for moveout velocity valid for homogeneous, isotropic media (Levin, 1971):

$$V_{\text{nmo}}(\phi) = V_{\text{nmo}}(0)/\cos\phi, \tag{30}$$

where $V_{\text{nmo}}(\phi)$ is the normal-moveout velocity for a reflector dipping at the angle ϕ, and $V_{\text{nmo}}(0)$ is the zero-dip NMO velocity. For homogeneous isotropic media, reflection moveout is purely hyperbolic, and equation (30) is exact for any spreadlength.

The discussion of dip-dependent NMO velocity given below is based on the analytic study of NMO velocities presented in Tsvankin (1995a). Let us consider a common-midpoint (CMP) gather over a homogeneous anisotropic medium with the CMP line perpendicular to the strike of the reflector (Figure 2). The only assumption made about anisotropy is that the incidence (sagittal) plane is a plane of symmetry. For instance, this treatment is valid for any plane containing the symmetry axis in transversely isotropic media (plus the isotropy plane), as well as for symmetry planes in orthorhombic media. Under this assumption, the normal-moveout velocity for all wave types can be expressed through the phase velocity V as (Tsvankin, 1995a)

$$V_{\text{nmo}}(\phi) = \frac{V(\phi)}{\cos\phi} \frac{\sqrt{1 + \dfrac{1}{V(\phi)} \dfrac{d^2V}{d\theta^2}}}{1 - \dfrac{\tan\phi}{V(\phi)} \dfrac{dV}{d\theta}}, \tag{31}$$

where the derivatives should be evaluated at the dip angle ϕ. Alkhalifah and Tsvankin (1995) generalize this equation for layered anisotropic media.

In the following, I concentrate on transversely isotropic media with a vertical symmetry axis (VTI media). The most convenient way to understand the influence of anisotropy on NMO velocity is to use the weak-anisotropy approximation. Using the weak-anisotropy equation for the P-wave phase velocity (13) and further linearizing in ε and δ yields

$$\frac{V_{\text{nmo}}(\phi)\cos\phi}{V_{\text{nmo}}(0)} = 1 + \delta \sin^2\phi + 3(\varepsilon - \delta)\sin^2\phi(2 - \sin^2\phi). \tag{32}$$

Equation (32) describes the anisotropy-induced distortions in the dip-dependence of P-wave NMO velocity. The P-wave dip-moveout error in transversely isotropic media can be split

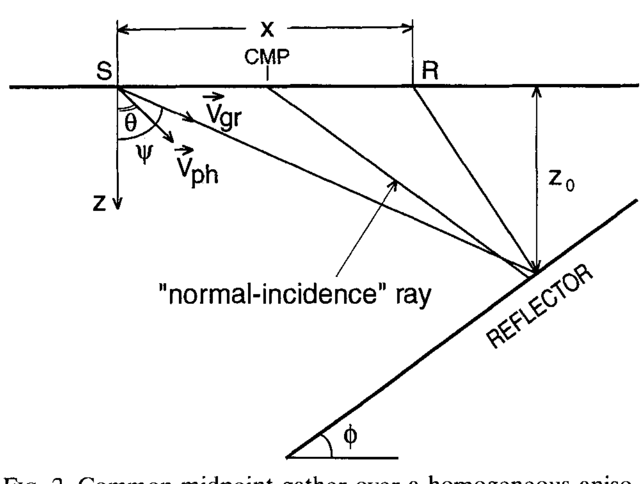

FIG. 2. Common-midpoint gather over a homogeneous anisotropic medium. $\vec{V}_{gr}$ and $\vec{V}_{ph}$ are the group and phase velocity vectors, respectively. The phase-velocity vector of the zero-offset ray (rather than the ray itself) is normal to the reflector.

into two major components, which may be called the "elliptical error" and "nonelliptical error." Since elliptical anisotropy corresponds to $\varepsilon = \delta$, the latter component is represented by the last term in expression (32). Analysis of the trigonometric coefficients in equation (32) shows that this nonelliptical term usually makes the most significant contribution to the total error. Thus, the difference $\varepsilon - \delta$ determines, to a large degree, the angular behavior of the *P*-wave NMO velocity. For typical positive values of the difference $\varepsilon - \delta$, the cosine-of-dip corrected moveout velocity is usually higher than the moveout velocity for a horizontal reflector.

Equation (32) gives a clear analytic explanation for the numerical results for specific transversely isotropic models reported in the literature (Levin, 1990). Note that the distortions of the isotropic cosine-of-dip dependence are not correlated with the magnitude of the *P*-wave velocity variations, which are usually determined by the value of ε.

What is the influence of the *S*-wave vertical velocity V_{S0} on the *P*-wave normal moveout velocity? If the reflector is horizontal, *P*-wave V_{nmo} depends just on V_{P0} and δ [equation (24)]. The weak-anisotropy approximation for the dip-dependent NMO velocity (32) does not contain V_{S0} either. However, from the phase-velocity equation (14) it is clear that V_{S0} does have an influence on the terms that are quadratic in ε and δ in the NMO equation (31).

Figure 3 shows the dependence of the *P*-wave NMO velocity on V_{S0} for several combinations of ε and δ, including those corresponding to uncommonly strong anisotropy. The NMO velocity in Figure 3 is multiplied with $\cos\phi$, as is conventionally done in the isotropic DMO correction. If the medium were isotropic, the cosine-of-dip corrected normal-moveout velocity would be independent of the dip angle. Because of the influence of the anisotropy, the corrected NMO velocity increases with dip.

For a representative range of V_{S0} in Figure 3, the influence of the *S*-wave vertical velocity is relatively weak. The maximum difference between the two extreme curves reaches about 7% at steep dips for the model with a large $\varepsilon = 0.5$, and $\delta = 0.1$. This is one of the rare cases when the term quadratic in the anisotropies (that contains V_{S0}) has a noticeable magnitude. For large $\varepsilon - \delta$ and large dips, the contribution of the anisotropy to the NMO velocity may even exceed the isotropic term. Indeed, for the model with $\varepsilon = 0.5$ and $\delta = 0.1$ (Figure 3), the anisotropic term

$$\frac{\tan\phi}{V(\phi)}\frac{dV}{d\theta}$$

in the denominator of the NMO equation (31) becomes large (on the order of 0.5) for steep reflectors. However, NMO velocities at large dips are so high that a variation in V_{nmo} of 7% would hardly change the traveltimes in a measurable way.

Figure 3 also shows that the influence of V_{S0} becomes more pronounced with increasing difference $\varepsilon - \delta$ and is relatively

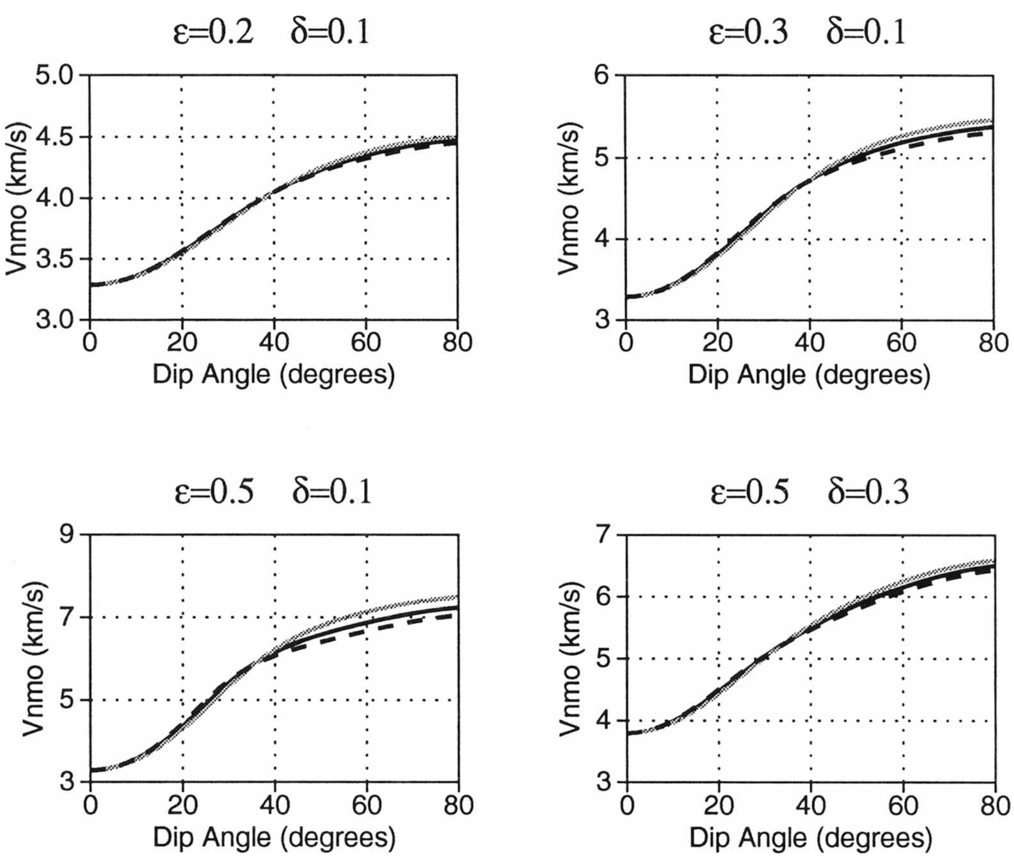

FIG. 3. The influence of V_{S0} on the cosine-of-dip corrected *P*-wave normal moveout velocity computed from formula (31). The dashed curve corresponds to $V_{P0}/V_{S0} = 1.5$, the black curve to $V_{P0}/V_{S0} = 1.75$, the gray curve to $V_{P0}/V_{S0} = 2.5$. $V_{P0} = 3$ km/s is the same on all plots.

insensitive to the individual values of the anisotropic parameters. On the whole, the contribution of V_{S0} to P-wave NMO velocities is insignificant and, for most practical purposes, can be ignored.

As pointed out above, in a homogeneous medium V_{P0} is just a scaling coefficient for the P-wave phase velocity, if ε and δ are kept constant. Therefore, V_{P0} does not change the dependence of the P-wave normal moveout velocity V_{nmo} on the dip angle ϕ.

The influence of ε and δ on the P-wave NMO velocity is illustrated in Figures 4 and 5. Each plot in these two figures contains three curves: the moveout velocity determined from $t^2 - x^2$ functions [calculated using Larner's (1993) ray-tracing code] using a spreadlength equal to the distance from the CMP to the reflector (solid); the exact analytic normal moveout velocity computed from equation (31) (dotted); and the weak-anisotropy approximation for V_{nmo} (dashed). Comparison between the first two curves makes it possible to estimate the influence of nonhyperbolic moveout on the moveout velocity for a typical-length spread. The difference between the second and third curves shows the error of the weak-anisotropy approximation.

If $\varepsilon - \delta$ is positive (the most common case, Figure 4), the anisotropy causes a pronounced increase in the cosine-of-dip corrected moveout velocity with dip angle. Even for relatively small $\varepsilon - \delta = 0.1$ (not shown here), the dip-moveout error reaches 25% at a 45° dip and 30–35% at a dip of 60°. For $\varepsilon - \delta = 0.2$ (Figure 4), the corrected moveout velocity at a 60° dip is consistently about 60% higher than the zero-dip moveout velocity!

For elliptically anisotropic models ($\varepsilon - \delta = 0$), shown for comparison in Figure 5, the DMO error is moderate: the difference between the corrected moveout velocity and the zero-dip V_{nmo} for $\phi < 60°$, $|\varepsilon| < 0.2$, and $|\delta| < 0.2$ is less than 15%.

Figures 4 and 5 demonstrate that the P-wave DMO signature is controlled, to a significant degree (but not entirely), by the difference $\varepsilon - \delta$. The dominant role of $\varepsilon - \delta$ is particularly pronounced for the most typical case $\varepsilon - \delta > 0$.

The weak-anisotropy approximation for the NMO velocity is sufficiently accurate for small and moderate values of ε and δ. The error of the weak-anisotropy result (as compared with the exact NMO velocity) does not exceed 5% for $|\varepsilon| \le 0.2$, $|\delta| \le 0.2$ (except for media with $\delta < -0.15$).

The above suite of plots also allows us to estimate the moveout-velocity distortions at various dips caused by nonhyperbolic moveout. Note that the difference between the moveout velocity on a finite spread and the NMO velocity changes

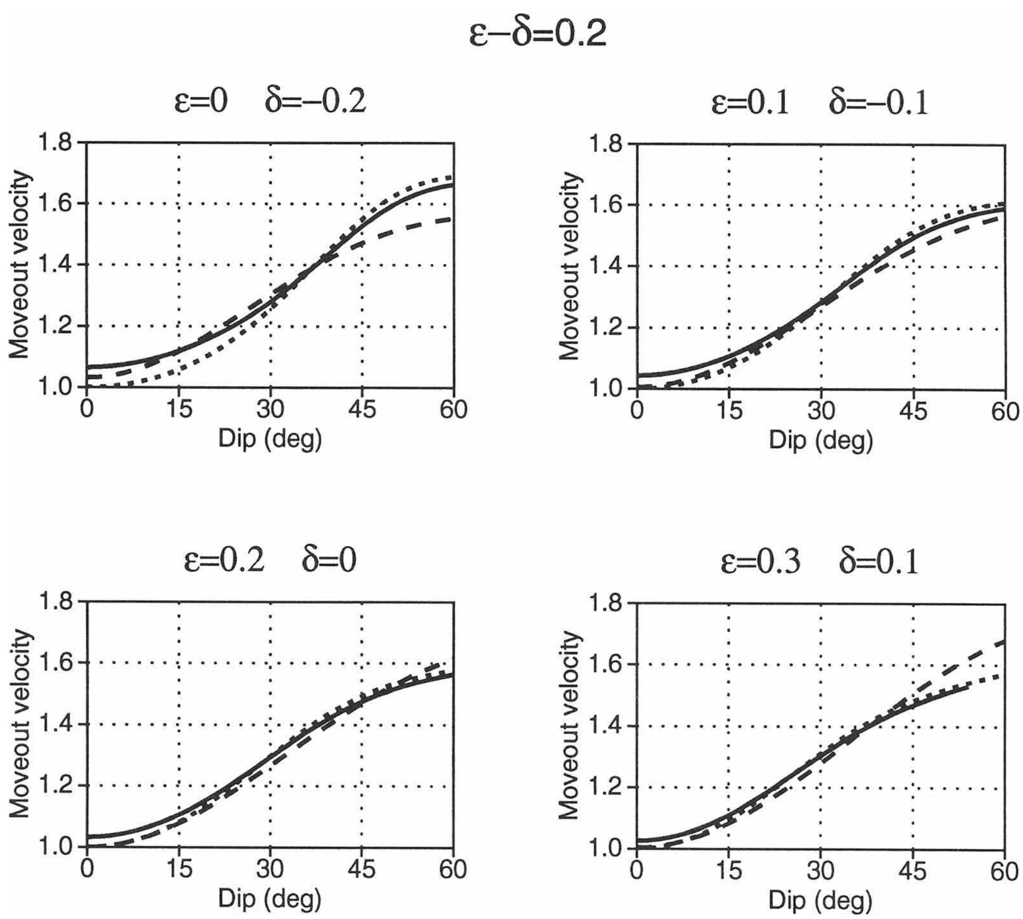

FIG. 4. Cosine-of-dip corrected P-wave moveout velocity for models with $\varepsilon - \delta = 0.2$. The solid curve is the moveout velocity calculated from $t^2 - x^2$ functions over a spreadlength equal to the distance from the CMP to the reflector; the dotted curve is the exact NMO velocity from formula (31); and the dashed curve is the weak-anisotropy approximation. All curves are normalized by the exact value of $V_{\text{nmo}}(0)$.

sign with increasing dip. It should be emphasized that the influence of nonhyperbolic moveout for steep reflectors is typically smaller than for zero dip. We conclude that if $|\epsilon - \delta| < 0.15$ to 0.2, nonhyperbolic moveout does not seriously distort the *P*-wave moveout velocity on typical-length spreads.

NMO velocity as a function of ray parameter

In the above analysis, we examined the NMO velocity as a function of the dip angle ϕ. However, since reflection data do not carry any explicit information about the dip angle, for the purposes of seismic processing and inversion $V_{\rm nmo}$ should be expressed through the ray parameter $p(\phi)$ corresponding to the zero-offset reflection:

$$p(\phi) = \frac{1}{2}\frac{dt_0}{dx_0} = \frac{\sin\phi}{V(\phi)}, \tag{33}$$

where $t_0(x_0)$ is the two-way traveltime on zero-offset data.

The replacement of the angle ϕ by the ray parameter p (horizontal slowness) can be done in a straightforward fashion using the phase-velocity equations for transverse isotropy. The NMO velocity (31) as a function of ray parameter for weak transverse isotropy reduces to (Alkhalifah and Tsvankin, 1995)

$$V_{\rm nmo}(p) = \frac{V_{\rm nmo}(0)}{\sqrt{1-y}}\,[1 + (\epsilon - \delta) f(y)], \tag{34}$$

where

$$f(y) \equiv \frac{y(4y^2 - 9y + 6)}{1 - y}, \qquad y \equiv p^2 V_{\rm nmo}^2(0);$$

Equation (34) is derived under the assumption that $y < 1$ (it is always true if the dip is not too steep). It is interesting to compare formula (34) with the corresponding weak-anisotropy NMO equation as a function of the dip angle (32). While the difference $\epsilon - \delta$ was emphasized as the most influential parameter in the NMO equation (32), $V_{\rm nmo}(\phi)$ does contain a separate contribution of δ. However, as $V_{\rm nmo}$ varies with the ray parameter, in the weak-anisotropy approximation it depends *only* on the combination $\epsilon - \delta$ and the zero-dip NMO velocity $V_{\rm nmo}(0)$.

Although equation (34) is valid for weak transverse isotropy, the numerical study in Alkhalifah and Tsvankin (1995) leads to similar results for transversely isotropic media with arbitrary strength of the anisotropy. The exact *P*-wave $V_{\rm nmo}(p)$ turns out to depend just on $V_{\rm nmo}(0)$ and the horizontal velocity $V_{P90} = V_{P0}\sqrt{1 + 2\epsilon}$. The velocities $V_{\rm nmo}(0)$ and V_{P90} can be combined to form a new effective parameter (Alkhalifah and Tsvankin, 1995)

$$\eta = \frac{1}{2}\left(\frac{V_{P90}^2}{V_{\rm nmo}^2} - 1\right) = \frac{\epsilon - \delta}{1 + 2\delta}, \tag{35}$$

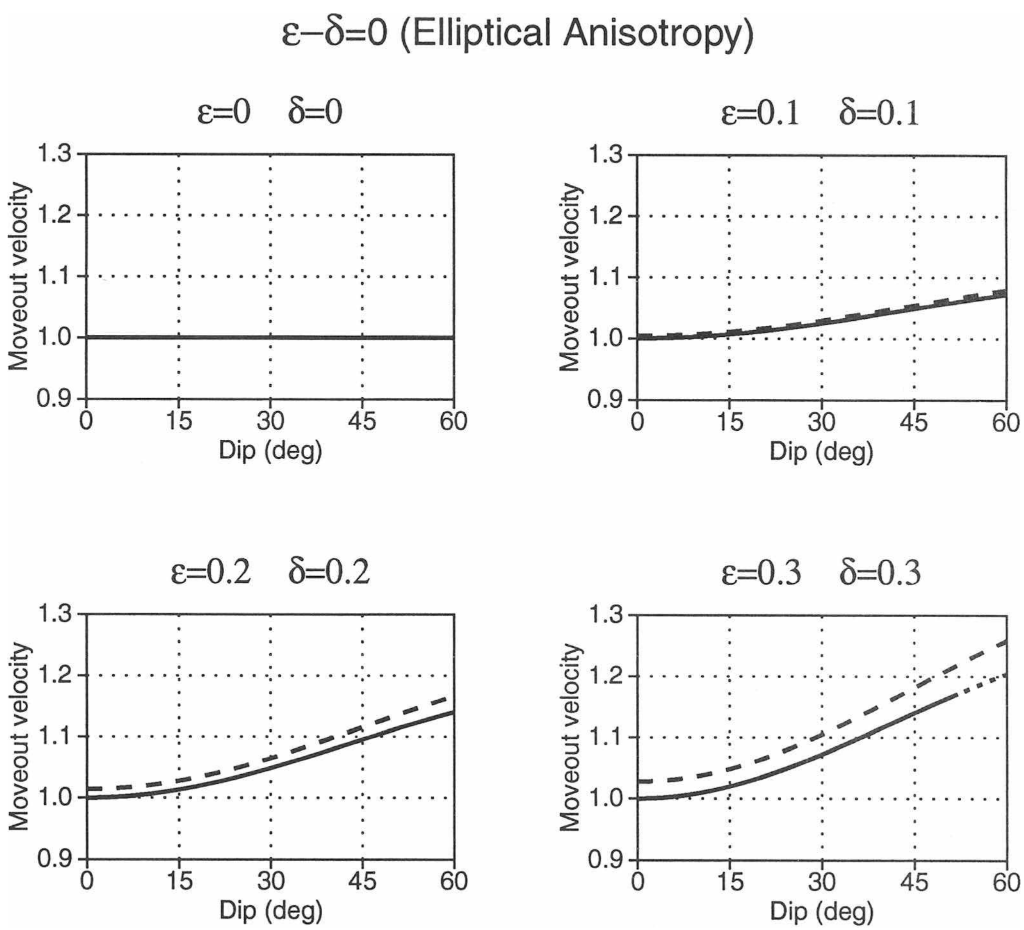

FIG. 5. Cosine-of-dip corrected *P*-wave moveout velocity for models with $\epsilon - \delta = 0$ (elliptical anisotropy).

which reduces to the difference $\varepsilon - \delta$ for weak anisotropy. Thus, *P*-wave NMO velocity can be represented as a function of just two parameters: the zero-dip velocity $V_{nmo}(0)$ and η. For elliptical anisotropy ($\varepsilon = \delta$, $\eta = 0$), NMO velocity is the same function of the ray parameter as in isotropic media.

This conclusion has important implications in the inversion of the dip-dependence of the NMO velocity for the anisotropic coefficients. The *P*-wave NMO velocities for two distinct dips provide enough information to recover the two effective parameters and reconstruct the NMO velocity as a function of ray parameter (Alkhalifah and Tsvankin, 1995). In the most common case when the zero-dip NMO velocity has been found by conventional NMO analysis, the moveout from a single dipping reflector makes it possible to recover the parameter η. Once $V_{nmo}(0)$ and η have been obtained, equation (31) can be used to reconstruct NMO velocity as a function of p and carry out DMO processing (Anderson and Tsvankin, 1994). Note that it is impossible to resolve the trade-off between V_{P0}, ε, and δ from *P*-wave NMO velocities, no matter how many dips are used.

Therefore, the effective parameters governing NMO velocities depend on the variable being used. *P*-wave NMO velocity as a function of the ray parameter is controlled by η, i.e., by the *normalized* difference $\varepsilon - \delta$. However, as shown in the previous section, if NMO velocity varies with the dip angle, the effective parameter (especially for positive $\varepsilon - \delta$) is just $\varepsilon - \delta$, without any normalization.

The importance of the family of models with the same $V_{nmo}(0)$ and η will be discussed in more detail after the description of nonhyperbolic moveout.

Dip dependence of NMO velocity in vertically inhomogeneous media

Next, let us consider the so-called "factorized" transversely isotropic (FTI) media with linear variation in vertical velocity with depth using the results in Tsvankin (1995a) and Larner (1993). In terms of the notation used here, the velocity V_{P0} in this model linearly increases with depth, while the V_{P0}/V_{S0} ratio and the anisotropic coefficients ε and δ remain constant. The moveout velocity is calculated from $t^2 - x^2$ curves generated using Larner's (1993) ray-tracing algorithm (Figure 6).

Comparison of Figure 6 with Figure 4 shows that for typical positive values of $\varepsilon - \delta$, angular variations of the cosine-of-dip corrected moveout velocity are substantially suppressed by the velocity gradient, and the accuracy of the simplest constant-velocity DMO formula (30) is satisfactory. This means that for FTI models with $\varepsilon - \delta > 0$ and a typical (positive) vertical velocity gradient, the DMO correction that ignores both anisotropy and inhomogeneity is often more accurate than a $V(z)$ DMO that ignores anisotropy.

Another important conclusion from Figure 6 is that in factorized, vertically inhomogeneous VTI media, the *P*-wave moveout velocity is still primarily controlled by the difference between ε and δ, rather than by the individual values of these parameters. However, in $V(z)$ media, dip-dependence of the moveout velocity is also a function of the velocity gradient, the rms vertical velocity, and the depth of the reflector. The influence of the shear-wave vertical velocity on the *P*-wave NMO velocity in FTI media remains insignificant.

Nonhyperbolic reflection moveout

The standard hyperbolic approximation for reflection moveouts in inhomogeneous media is accurate only for relatively short spreads, even in the absence of anisotropy. Angle-dependent velocity makes reflection moveout nonhyperbolic even in a horizontal homogeneous layer. Here, I use the results of Tsvankin and Thomsen (1994) and Hake et al. (1984) to examine nonhyperbolic moveout in a horizontally homogeneous, transversely isotropic medium with a vertical symmetry axis. An alternative way of treating nonhyperbolic moveout was developed by Dellinger and Muir (1993) who suggested expressing reflection traveltime in horizontally layered anisotropic media as a power series in terms of ray parameter using an equivalent-medium theory.

Qualitative description of nonhyperbolic moveout on "intermediate" spreads (offset-to-depth ratio $x/z < 1.7 - 2$) can be given in terms of the quartic Taylor series expansion (20). The quartic moveout term for a single transversely isotropic layer with arbitrary strength of the velocity anisotropy is (Tsvankin and Thomsen, 1994):

$$A_4 = -\frac{2(\varepsilon - \delta)}{t_{P0}^2 V_{P0}^4} \frac{1 + 2\delta/f}{(1 + 2\delta)^4}, \tag{36}$$

where $f = 1 - V_{S0}^2/V_{P0}^2$ [equation (8)]. Clearly, the influence of the *S*-wave vertical velocity V_{S0} on the quartic term (36) is relatively weak because, as before, V_{S0} is contained only in the term quadratic in the anisotropies ε and δ.

Deviations from hyperbolic moveout can be measured by the relative magnitude of the quartic term as a function of the normalized offset $\bar{x} = x/2z$:

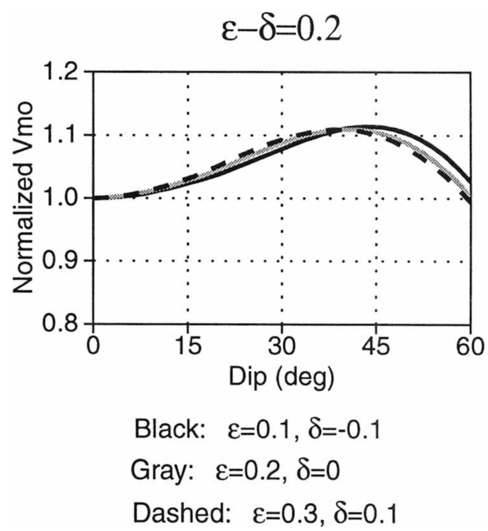

FIG. 6. *P*-wave moveout velocity corrected for the cosine of the dip angle for VTI models with $\varepsilon - \delta = 0.2$ and a velocity gradient of $0.6\,s^{-1}$. The curves are normalized by the moveout velocity for a horizontal reflector. Each curve corresponds to a different pair of ε, δ. The distance from the CMP to the reflector and the spreadlength are 3000 m; the rms vertical velocity down to 3000 m is 3500 m/s.

$$\frac{A_4 x^4}{A_0 + A_2 x^2} = -\bar{x}^4 \frac{2(\varepsilon - \delta)}{(1+2\delta)^4} \frac{1 + \dfrac{2\delta}{f}}{1 + \dfrac{\bar{x}^2}{1+2\delta}}. \quad (37)$$

The strength of the *P*-wave nonhyperbolic moveout is proportional to the magnitude of the difference $\varepsilon - \delta$, i.e., to deviations from the elliptical model. If anisotropy is elliptical ($\varepsilon = \delta$), moveout is purely hyperbolic. For fixed $\varepsilon - \delta$ and conventional (small negative or positive) δ, deviations from nonhyperbolic moveout increase with *decreasing* δ. Hence, there is no simple correlation between the degree of velocity anisotropy and nonhyperbolic moveout.

The quartic moveout equation rapidly loses accuracy with increasing offset and should be replaced by a more accurate moveout formula as presented in Tsvankin and Thomsen (1994):

$$t^2(x) = t_{P0}^2 + A_2 x^2 + \frac{A_4 x^4}{1 + A x^2}, \quad (38)$$

where

$$A = \frac{A_4}{\dfrac{1}{V_{P90}^2} - A_2},$$

and V_{P90} is the horizontal velocity.

Equation (38) is valid not only for the single-layer model but also for stratified transversely isotropic media, provided the appropriate coefficients A_2, A_4, and A are used. Tsvankin and Thomsen (1994) show that the moveout formula (38) remains numerically accurate for long spreads (2–3 times, and more, the reflector depth) and for pronounced anisotropy.

Since the *P*-wave horizontal velocity V_{P90} and the quadratic moveout term A_2 are independent of the *S*-wave vertical velocity, V_{S0} can change *P*-wave moveout (38) only through the quartic coefficient A_4, but this influence is practically negligible.

Let us now rewrite the moveout equation (38) using the effective parameters $V_{\text{nmo}}(0)$ and η suggested in Alkhalifah and Tsvankin (1995). Substituting $V_{\text{nmo}}(0)$ and η into formula (38) and ignoring the contribution of V_{S0} to the quartic term A_4, we obtain

$$t^2(x) = t_{P0}^2 + \frac{x^2}{V_{\text{nmo}}^2(0)} - \frac{2\eta x^4}{V_{\text{nmo}}^2(0)[t_{P0}^2 V_{\text{nmo}}^2(0) + (1+2\eta)x^2]}. \quad (39)$$

Thus, *P*-wave long-spread moveout is determined just by the vertical traveltime and two effective parameters—$V_{\text{nmo}}(0)$ and η, with no separate dependence on V_{P0}, ε, or δ. If $\eta = 0$, the medium is elliptical and the moveout is purely hyperbolic.

To use equation (38) in the description of nonhyperbolic moveout for horizontally layered VTI media, the quadratic (A_2) and quartic (A_4) moveout coefficients and V_{P90} should be calculated for the stack of layers above the reflector. Tsvankin and Thomsen (1994) show how the coefficients A_2, A_4, and V_{P90} for a layered medium can be determined from the values of A_2, A_4, and V_{P90} in the individual layers. Since the single-layer coefficients A_2, A_4, and V_{P90} are functions of the two effective parameters $V_{\text{nmo}}(0)$ and η, the *P*-wave moveout curve for a layered medium depends on the values of $V_{\text{nmo}}(0)$ and η averaged in a complicated fashion over the stack of layers.

Although equations (38) and (39) describe moveout for a horizontal reflector, they also can be regarded as the diffraction curves, accurate to a certain dip on the zero-offset (or stacked) section. Since time migration is based on collapsing such diffraction curves to their apex, the values of $V_{\text{nmo}}(0)$ and η should be sufficient to generate an accurate poststack time-migration impulse response (at least, up to a certain dip). Alkhalifah and Tsvankin (1995) show that both poststack and prestack time migration in VTI media are indeed fully controlled by the parameters $V_{\text{nmo}}(0)$ and η. *Depth* migration will still produce depth errors if the value V_{P0} is inaccurate, but this is a different issue.

POLARIZATION VECTOR

The vector of particle motion, or the polarization vector, plays an important role in the processing and interpretation of multicomponent VSP and crosshole surveys. Also, deviations of the polarization vector from its "isotropic" direction may cause distortions of radiation patterns in anisotropic media (discussed in more detail in the next section).

To obtain the polarization vector, we have to substitute the expression for a steady-state plane wave into the wave equation and solve the resulting simultaneous equations (the so-called Christoffel equations), which involve the components of the slowness and displacement vectors. For *P*- and *SV*-waves in the $[x_1, x_3]$ plane of a transversely isotropic medium (the x_3-direction coincides with the symmetry axis), the Christoffel equations reduce to (Musgrave, 1970)

$$G_{11}U_1 + G_{13}U_3 = 0, \quad (40)$$

$$G_{13}U_1 + G_{33}U_3 = 0, \quad (41)$$

where U_1 and U_3 are the components of the displacement vector, and G is the Christoffel matrix. The components of the Christoffel matrix can be expressed in terms of phase velocity as follows:

$$G_{11} = c_{11}\frac{\sin^2\theta}{V^2} + c_{44}\frac{\cos^2\theta}{V^2} - \rho,$$

$$G_{33} = c_{44}\frac{\sin^2\theta}{V^2} + c_{33}\frac{\cos^2\theta}{V^2} - \rho,$$

$$G_{13} = (c_{13} + c_{44})\frac{\sin\theta\cos\theta}{V^2}.$$

For the *P*- or *SV*-wave phase velocity, $G_{11}G_{33} = G_{13}^2$, and either of equations (40) or (41) can be used to find the polarization direction. Substituting G_{11}, G_{33}, and G_{13} into (40) or (41), we obtain the polarization angle γ as

$$\tan\gamma \equiv \frac{U_1}{U_3} = \frac{\sin\theta\cos\theta\,(c_{13} + c_{44})}{\rho V^2 - c_{11}\sin^2\theta - c_{44}\cos^2\theta}. \quad (42)$$

Equation (42) is valid for any strength of the anisotropy.

Using the weak-anisotropy approximation for the phase velocity (13) and carrying out further linearization in ε and δ, we get a concise expression for the *P*-wave polarization angle:

$$\tan \gamma = \tan \theta\{1 + B[2\delta + 4(\varepsilon - \delta) \sin^2 \theta]\}, \quad (43)$$

$$B \equiv \frac{1}{2f} = \frac{1}{2(1 - V_{S0}^2/V_{P0}^2)}.$$

If a *P*-wave is generated by a point source, the polarization at any receiver location can be obtained by applying equation (43) at the phase angle corresponding to the group (source-receiver) direction.

Thomsen (1986) showed that for weak anisotropy $\cos(\gamma - \theta)$ differs negligibly from unity. However, since $\cos(\gamma - \theta) = 1 - O[(\gamma - \theta)^2]$, it does *not* follow that $(\gamma - \theta)$ itself differs negligibly from zero, i.e., it is not true that the deviation of the polarization angle from the phase angle can be ignored (Rommel, 1994).

In fact, the *P*-wave polarization angle is closer to the group angle than to the phase angle. The weak-anisotropy expressions for the *P*-wave group (19) and polarization (43) angles are quite similar; the difference between the two is in the quantity B, which is dependent on the V_{P0}/V_{S0} ratio. Since for plausible values of V_{P0}/V_{S0}, B satisfies $0.5 < B < 1$, the polarization vector lies between the phase and group-velocity vectors, usually being closer to the group vector. This analytic result is in good agreement with the numerical analysis of *P*-wave polarizations given in Tsvankin and Chesnokov (1990a), who show that the *P*-wave polarization and group-velocity vectors usually remain close to each other even in more complicated orthorhombic models.

Unlike the weak-anisotropy formulas for the *P*-wave phase and NMO velocity, equation (43) does depend on the shear-wave vertical velocity through the parameter B. Variation in V_{S0} within a realistic range can cut the *P*-wave polarization anomaly (i.e., the difference between the group and polarization angles) in half (Figure 7). However, since the anomaly as a whole is small, the influence of V_{S0} on the *P*-wave polarization angle for moderate anisotropies $|\varepsilon| \le 0.2$, $|\delta| \le 0.2$ is weak.

The analysis above is valid for typical transversely isotropic media with $c_{13} + c_{44} > 0$. Helbig and Schoenberg (1987) show that for "abnormal" media that have negative $c_{13} + c_{44}$, the *P*-wave polarization vector may even become perpendicular to the phase-velocity vector.

DYNAMIC PROPERTIES

Radiation pattern

The shape of body-wave radiation patterns is important in many applications both in earthquake seismology and seismic exploration. Here, I follow Tsvankin (1995b) to discuss the influence of anisotropic radiation patterns on amplitude variation with offset (AVO) analysis—one of the few exploration methods capable of direct detection of hydrocarbons. It is now well known that the angular dependence of reflection coefficients may be significantly distorted in the presence of elastic anisotropy (Banik, 1987; Wright, 1987). Yet another distortion of AVO signatures (e.g., of AVO gradient) results from the influence of anisotropy on the distribution of energy along the wavefront of the wave traveling down to the reflector and back up to the surface (Figure 8), a transmission effect completely independent of the reflector. Significant anisotropy above the target horizon may be rather typical of sand-shale sequences commonly encountered in AVO analysis (Kim et al., 1993).

Far-field, point-source radiation in isotropic homogeneous, nonattenuating media is determined just by the source directivity factor and spherical divergence of amplitude (Aki and Richards, 1980). The far-field approximation for source radiation in anisotropic media (Tsvankin and Chesnokov, 1990a; Ben-Menahem et al., 1991; Gajewski, 1993), is a much more complicated function that depends on the shape of the slowness surface. The most significant distortion of radiation patterns in anisotropic media is caused by the phenomenon defined in Tsvankin and Chesnokov (1990a) as "focusing" and "defocusing" of energy. Energy increases (focuses) in parts of the wavefront with a high concentration of group-velocity vectors of elementary plane waves (which comprise point-source radiation). Conversely, defocusing corresponds to areas with a low concentration of group-velocity vectors. Often (but not always), focusing takes place near velocity maxima, while defocusing is often associated with velocity minima.

Tsvankin (1995b) shows that the far-field radiation pattern of *P*-, *SV*-, or *SH*-waves from a point force for weak transverse isotropy ($|\varepsilon| \ll 1$, $|\delta| \ll 1$, $|\gamma| \ll 1$) reduces to

$$U(R, \theta) = \frac{F_u(\gamma)}{4\pi\rho V^2(\theta) R} \frac{1}{\sqrt{\frac{\sin \psi}{\sin \theta}} \left(1 + \frac{1}{V}\frac{d^2V}{d\theta^2}\right)}, \quad (44)$$

where U is the magnitude of the displacement, V is the phase velocity, $R = \sqrt{z^2 + r^2}$ (z is the receiver depth, r is the horizontal source-receiver offset), and the source term F_u is projection of the force on the displacement (polarization) vector. Equation (44) does not take the influence of the free surface into account. This equation should be evaluated at the phase angle θ, corresponding to a given ray (group-velocity) angle $\psi = \tan^{-1}(r/z)$ of the incident wave; both angles are measured from the symmetry axis.

Formula (44) demonstrates how point-source radiation is distorted by velocity anisotropy. The leading term $F_u(\gamma)/$

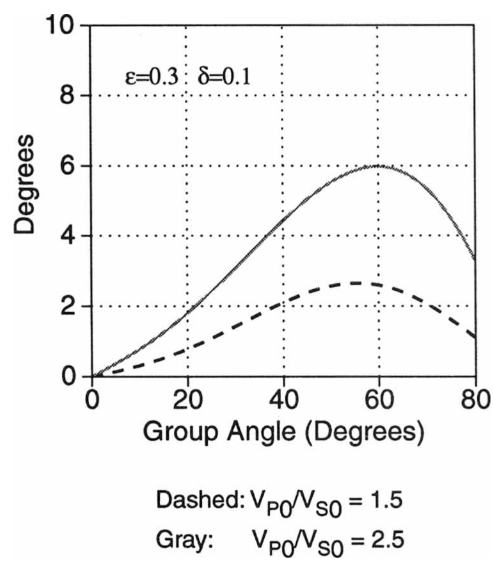

FIG. 7. The difference between *P*-wave group and polarization angles (exact computation) for a model with $\varepsilon = 0.3$, $\delta = 0.1$, and two values of V_{P0}/V_{S0} ratio. The angles are measured from the symmetry axis.

$(4\pi\rho V^2 R)$ formally coincides with the well-known expression for the far-field, point-force radiation in isotropic media (Aki and Richards, 1980). However, the phase velocity in equation (44) is angle-dependent; also, the source term F_u may be distorted by the anisotropy because the polarization direction deviates from the ray direction. The term under the radical represents the pure contribution of the anisotropy to the radiation pattern.

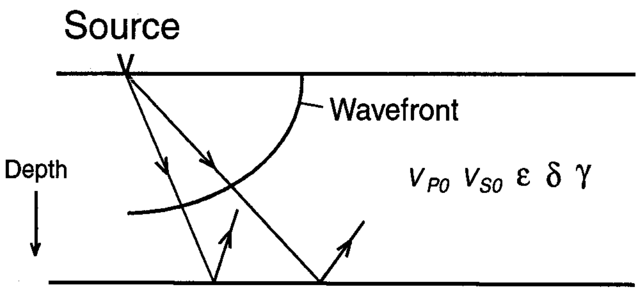

FIG. 8. Reflection from the bottom of a transversely isotropic layer. Anisotropy distorts the distribution of energy along the wavefront of the incident wave.

Further linearization of equation (44) in the anisotropic parameters ε and δ leads to the following expression for the *P*-wave:

$$U_P(R, \theta) = \frac{F_u(\gamma)}{4\pi\rho V_{P0}^2 R} \frac{1 - 2(\varepsilon - \delta)\sin^2 2\theta + \delta \sin^2 \theta}{1 + 2\delta}. \tag{45}$$

From formula (45) it is clear that transverse isotropy distorts the amplitude even in the symmetry direction ($\theta = 0$). Moreover, by using the stationary-phase expression in Tsvankin and Chesnokov (1990a), it can be shown that the weak-anisotropy approximation (45) is exact (in the far-field) for $\theta = 0$. The distortion of the *P*-wave amplitude in the symmetry direction depends on just one anisotropic coefficient $-$ δ. If $\delta < 0$, the velocity function has a maximum at $\theta = 0°$, and the amplitude in the symmetry direction increases because of the focusing of energy; conversely, if $\delta > 0$, a velocity minimum leads to lower amplitude at $\theta = 0°$ because of the defocusing.

The above equations for the radiation pattern are derived for an unbounded medium and, therefore, can be used for any orientation of the symmetry axis. Assuming that the symmetry axis is vertical, angular amplitude distortions near the symmetry direction are of most concern in AVO analysis. Equation (45) shows that the lowest-order anisotropic angular correction to the radiation pattern near the symmetry axis is determined

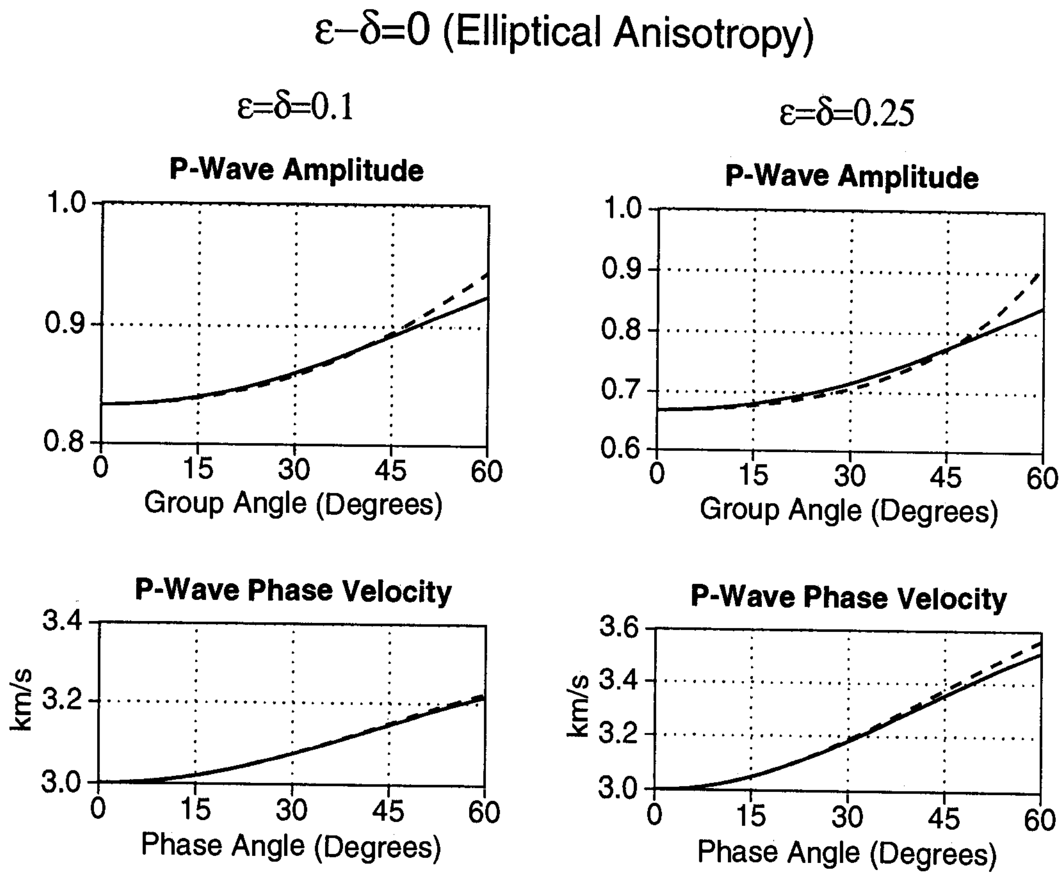

FIG. 9. Normalized *P*-wave amplitude from a force parallel to the symmetry axis for models with $\varepsilon - \delta = 0$ (elliptical anisotropy). The solid curve is the far-field amplitude calculated by the stationary phase method; the dashed curve is the weak-anisotropy approximation (45). The amplitude curves are normalized by the radiation pattern in the corresponding isotropic model ($\varepsilon = 0$, $\delta = 0$). The plots at the bottom show the exact phase velocity (solid curve) and its weak-anisotropy approximation (13) (dashed curve).

by the difference $\varepsilon - \delta$. For elliptical anisotropy ($\varepsilon = \delta$), the term $2(\varepsilon - \delta)\sin^2 2\theta$ vanishes, and the anisotropic angular correction reduces to $\delta \sin^2 \theta$. Therefore, the distortions of the shape of the radiation pattern in this case (given by $\delta \sin^2 \theta$) are relatively small between 0° and 40°, unless δ is unusually large.

Angular distortions of the radiation pattern may also be caused by the source term $F_u(\gamma)$, which depends on the polarization vector [equations (42) and (43)]. However, for moderate ε and δ ($|\varepsilon| \leq 0.2$, $|\delta| \leq 0.2$), the influence of anisotropy on the point-force directivity factor F_u in the angular range 0–40° is limited to a few percent. For other sources, such as dislocations or explosions, the dependence of the source term on anisotropy is more complicated, and can make a more significant contribution to the distortions of the angular amplitude distribution (Tsvankin and Chesnokov, 1990b).

Clearly, the influence of transverse isotropy on P-wave amplitudes is determined mostly by ε and δ. However, P-wave radiation pattern also depends on the velocities V_{P0} and V_{S0}. While the P-wave velocity V_{P0} is just a scaling coefficient, the situation with the velocity ratio V_{P0}/V_{S0} looks more complicated. As we have seen in the previous sections, the influence of the S-wave vertical velocity on P-wave phase and group velocities is practically negligible, even for strong anisotropy. The amplitude, however, depends not just on phase velocity and its derivatives, but also on the components of the Christoffel matrix. Nonetheless, as shown in Tsvankin (1995b), not only the velocity but also the far-field amplitude of the P-wave is practically independent of the S-wave vertical velocity.

Figures 9 and 10 display P-wave radiation patterns from a force parallel to the symmetry axis. The amplitude is calculated using the stationary-phase expression from Tsvankin and Chesnokov (1990a) valid in the far-field (solid curve), and the weak-anisotropy approximation (45) (dashed curve). Both curves are normalized by the radiation pattern in the corresponding isotropic medium ($\varepsilon = 0$, $\delta = 0$).

In elliptically anisotropic media with positive $\varepsilon = \delta$ (Figure 9), the normalized amplitude increases with angle, but the amplitude variations in the angular range 0°–40° remain mild, even for models with significant velocity anisotropy. This conclusion is confirmed by the exact analytic expression for radiation patterns in elliptically anisotropic media (Ben-Menahem, 1990; Tsvankin, 1995b).

For models with $\varepsilon - \delta > 0$, believed to be typical for subsurface formations, transverse isotropy may cause the P-wave amplitude to drop by 30% and more over the first 40° from the symmetry direction (Figure 10). If the difference $\varepsilon - \delta$ is positive, the influence of the anisotropy becomes stronger with increasing $\varepsilon - \delta$ and, for fixed $\varepsilon - \delta$, with decreasing values of ε and δ. Thus, there is no direct correlation between the strength of the velocity anisotropy and the amplitude anomalies.

The weak-anisotropy approximation for P-wave radiation (45) is closer to the exact solution for models with $\varepsilon \leq \delta$ than for media with positive $\varepsilon - \delta$. Still, for models with typical $0 < \varepsilon - \delta < 0.2$, the accuracy of the weak-anisotropy approximation is sufficiently high.

Reflection coefficient

The presence of elastic anisotropy on either side of the reflector may significantly distort the angular dependence of reflection coefficients. Analytic approximations for reflection

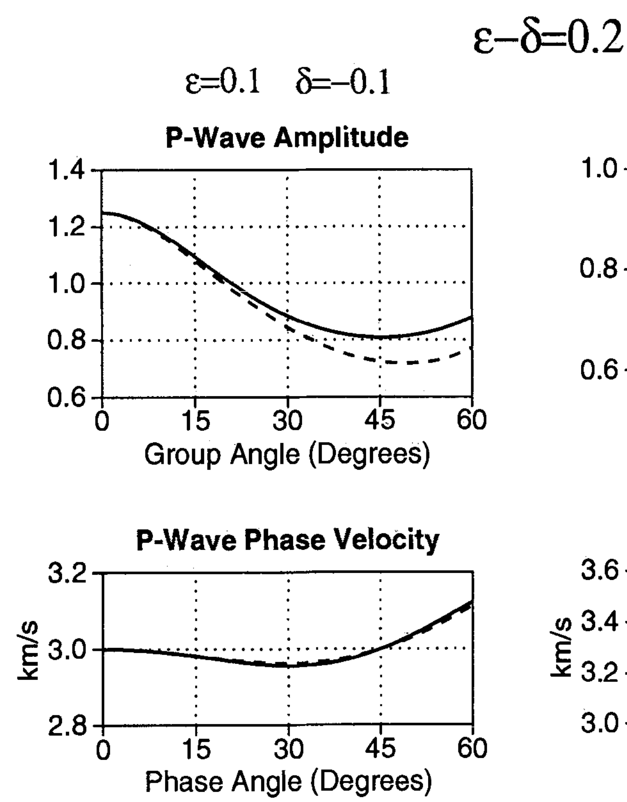

FIG. 10. Normalized P-wave amplitude from a force parallel to the symmetry axis for models with $\varepsilon - \delta = 0.2$.

coefficients at a boundary between two transversely isotropic media with a vertical symmetry axis were developed by Banik (1987) and Thomsen (1993). In the limit of weak anisotropy and of small velocity and density contrasts across the reflector, the *P*-wave reflection coefficient is given by (Thomsen, 1993):

$$R(\theta) = R_{\text{isot}}(\theta) + R_{\text{anis}}(\theta), \qquad (46)$$

where $R_{\text{isot}}(\theta)$ is the reflection coefficient in the absence of anisotropy ($\varepsilon = 0$, $\delta = 0$), and

$$R_{\text{anis}}(\theta) = \frac{1}{2}(\delta_2 - \delta_1)\sin^2\theta + \frac{1}{2}(\varepsilon_2 - \varepsilon_1)\sin^2\theta\tan^2\theta. \qquad (47)$$

Equation (47) is presented here in the corrected form given in Rüger (1995). Subscripts 1 and 2 refer to the media above and below the reflector, respectively. One of the convenient features of equations (46) and (47) is the separation of the "isotropic" and "anisotropic" parts of the reflection coefficient. Unlike Banik's (1987) approximation, formula (47) is not restricted to small incidence angles.

In contrast with the radiation pattern, the reflection coefficient at normal incidence is not distorted by transverse isotropy, i.e., $R_{\text{anis}} = 0$ if $\varepsilon = \delta = 0$. Note that the lowest-order angular correction to the reflection coefficient depends only on the change in δ across the reflector (no dependence on ε), while the lowest-order angular term in the radiation pattern (45) contains the difference between ε and δ. For examples of *P*-wave reflection coefficients at the boundary between transversely isotropic shales and isotropic sands, see Kim et al. (1993).

It should be emphasized that the influence of the *S*-wave vertical velocity V_{S0} on the *P*-wave reflection coefficient is limited to the isotropic term $R_{\text{isot}}(\theta)$, at least for weak transverse isotropy. The anisotropic correction to the reflection coefficient, derived in the weak-anisotropy approximation, is entirely independent of V_{S0}.

In AVO analysis, it is important to compare the distortions of the *P*-wave radiation pattern with the influence of transverse isotropy on the reflection coefficient. Obviously, it is difficult to make a general comparison, because angular variations in the reflection coefficient depend on the difference in the anisotropic parameters across the reflector, while the radiation pattern is entirely determined by the properties of the incidence medium. Also, the influence of anisotropy on the reflection coefficient depends on the impedance contrast, i.e., it is more pronounced for weak reflectors. However, Tsvankin (1995b) shows that the distortions of the radiation pattern and reflection coefficient often are of the same order of magnitude. For "bright spots" with a large amplitude of the normal-incidence reflection and a relatively slow variation in the absolute value of the reflection coefficient with angle, amplitude distortions above the reflector may even reverse the sign of the AVO gradient.

DISCUSSION: NOTATION

A proper choice of parameterization was very important to this study. Here, I have used the notation for transversely isotropic media developed by Thomsen (1986). Some advantages of the Thomsen parameters, explained in his original paper, were discussed further in the introduction. A major misconception about Thomsen notation that still persists in the literature is that it is useful only for weak anisotropy. This work shows that application of the Thomsen parameters is helpful in solving a wide range of practically important seismological problems in transversely isotropic media with any strength of velocity anisotropy. The results of this paper, which support this conclusion, can be summarized as follows:

1) It is possible to cut down on the number of independent parameters needed to describe *P*-wave propagation because the shear-wave vertical velocity V_{S0} has a weak (usually negligible) influence on *P*-wave signatures, even in media with strong velocity variations. Although the *P*-wave reflection coefficient does depend on the jump in V_{S0} across the interface, the contribution of transverse isotropy to the reflection coefficient is practically independent of V_{S0}. Therefore, the influence of transverse isotropy on *P*-wave propagation is controlled just by the *P*-wave vertical velocity V_{P0} and two anisotropic coefficients, ε and δ, with V_{P0} being no more than a scaling coefficient in homogeneous media. This facilitates our understanding of anisotropic wave propagation and implementation of inversion and processing algorithms in transversely isotropic media.
2) Traveltime inversion of *P*-wave data using the conventional notation is always ambiguous because the trade-off between the parameters c_{13} and c_{44} can never be resolved, unless some independent information about one of these coefficients is available. This ambiguity is explained by the fact that c_{13} and c_{44} contribute to *P*-wave phase and group velocity only through the parameter δ.
3) Not just NMO velocity [as shown in Thomsen's (1986) paper], but also the phase velocity (a fundamentally important function), the quartic moveout coefficient, and nonhyperbolic *P*-wave moveout for horizontal reflectors can be expressed concisely through the anisotropic parameters ε and δ. These analytic developments are valid for arbitrary strength of the anisotropy.
4) The coefficients ε, δ, and γ are well-suited for developing the weak-anisotropy approximation for a wide range of seismic signatures, including body-wave amplitudes. Systematic application of the weak-anisotropy approximation provides valuable analytic insight into the influence of transverse isotropy on seismic wavefields.

This paper is devoted mostly to the generic *P*-wave signatures (such as phase velocity, polarization vector, and radiation pattern), as well as the signatures important in reflection seismology and vertical seismic profiling. Analysis and inversion of seismic data may require defining different effective parameters for specific acquisition geometries. For instance, *P*-wave traveltimes measured in crosswell surveys usually correspond to near-horizontal rays and, therefore, are weakly dependent on near-vertical velocity variations. While the exact phase-velocity equation (10) remains valid for any propagation angle, it is difficult to resolve the vertical velocity V_{P0} and the parameter δ (assuming a vertical symmetry axis) from crosswell measurements. In this case, it may be more useful to parameterize the medium by the horizontal velocity and a combination of the anisotropic parameters responsible for the phase velocity variation near horizontal. However, a more comprehensive discussion of crosswell surveys is outside of the scope of this paper.

CONCLUSIONS

The description of P-wave signatures given in the paper included phase, group, and normal-moveout velocities, nonhyperbolic moveout, polarization vector, radiation pattern, and reflection coefficient. The analysis was based on a series of analytic solutions valid for transversely isotropic media with arbitrary strength of anisotropy (the only exception is the reflection coefficient, which was studied in the weak-anisotropy approximation). Although these solutions are convenient to implement numerically, some of them are not simple enough to elucidate the relation between various seismic phenomena and the parameters of the anisotropic velocity field. To gain insight into the influence of transverse isotropy on seismic signatures, I have applied the weak-anisotropy approximation systematically and checked its accuracy by comparing it with the exact solutions.

The influence of transverse isotropy on P-wave signatures is controlled by two dimensionless anisotropic parameters $-\varepsilon$ and δ, with the P-wave vertical velocity V_{P0} being a scaling coefficient, for homogeneous models. P-wave signatures of most interest in reflection seismology can be divided into two main groups. For the first group, that includes the normal-moveout velocity for horizontal reflectors, small-angle reflection coefficient, and point-force radiation in the vertical (symmetry) direction, the influence of transverse isotropy is entirely determined by the parameter δ.

The second group comprises the dip-dependence of NMO velocity, magnitude of nonhyperbolic moveout, time-migration impulse response, the shape of the radiation pattern in the angular range 0°–40°, and the subcritical reflection coefficient. The influence of transverse isotropy on these signatures is determined by both anisotropies (ε and δ) and (with the exception of the reflection coefficient) is primarily governed by the difference $\varepsilon - \delta$, i.e., by deviations from the elliptically anisotropic model. Because of the high sensitivity of P-wave signatures to $\varepsilon - \delta$, application of the elliptical-anisotropy approximation in P-wave processing may lead to unacceptable errors, even if the medium is relatively close to elliptical.

Therefore, the results for a wide range of seismic phenomena show that there is no apparent correlation between the strength of P-wave velocity anisotropy and the influence of transverse isotropy on reflection moveouts and amplitudes. The magnitude of the P-wave velocity variations is usually determined by the value of ε (unless $|\varepsilon|$ is much smaller than $|\delta|$), while signatures used in reflection seismology depend either just on δ or on both coefficients $-\varepsilon$ and δ (with the difference between the two coefficients being the most influential parameter). Therefore, the terms "weak anisotropy" or "strong anisotropy" are meaningless without a reference to a particular problem. For instance, while the model with $\varepsilon = 0.1$, $\delta = -0.1$ is weakly anisotropic in terms of velocity variations, it can be characterized as strongly anisotropic regarding the distortions of the P-wave radiation pattern.

As shown in Alkhalifah and Tsvankin (1995), the influence of vertical transverse isotropy on *time* processing is determined by the effective parameter $\eta = (\varepsilon - \delta)/(1 + 2\delta)$. The parameter η and the zero-dip, normal-moveout velocity $V_{nmo}(0)$ control the P-wave NMO velocity expressed as a function of the ray parameter, long-spread (nonhyperbolic) reflection moveout for a horizontal reflector, and poststack and prestack time-migration impulse responses. In principle, η can be replaced by other anellipticity parameters formed by combining the NMO velocity for a horizontal reflector $V_{nmo}(0)$ and the horizontal velocity. Alkhalifah and Tsvankin (1995) have developed an inversion procedure designed to obtain η and $V_{nmo}(0)$ from P-wave NMO velocities measured for two different dips. This inversion technique provides enough information to perform all essential time-processing steps including NMO correction, DMO processing, and time migration.

Thus, P-wave reflection moveout (including nonhyperbolic moveout on long spreads and NMO velocity from dipping refectors) depends just on $V_{nmo}(0)$ and η and, therefore, is insufficient to obtain the true vertical velocity required for time-to-depth conversion. In some cases, the vertical velocity can be determined directly if check shots or well logs are available. Then, dip-dependent P-wave NMO velocity can be used to obtain ε and δ. Other sources of additional information are the short-spread moveout velocities of SV or P-SV waves and long-spread SV-wave moveout (Tsvankin and Thomsen, 1995).

Although the discussion here was centered on vertical transverse isotropy, many analytic results in this paper (such as those for an unbounded homogeneous medium) are valid for any orientation of the symmetry axis.

ACKNOWLEDGMENTS

I am grateful to Leon Thomsen (Amoco) and Ken Larner (CSM) for helpful discussions and their critical reviews of the manuscript. I wish to thank Tariq Alkhalifah, Tagir Galikeev, and Andreas Rüger (all of CSM) and John Anderson (Mobil) for their contributions to this work. Review by Reinaldo Michelena (Intevep) helped to improve the paper. The support for this work was provided by the members of the Consortium Project on Seismic Inverse Methods for Complex Structures at the Center for Wave Phenomena, Colorado School of Mines, and by the United States Department of Energy, Grant Number DE-FG02-89ER14079 (this support does not constitute an endorsement by DOE of the views expressed in this paper).

REFERENCES

Aki, K., and Richards, P. G., 1980, Quantitative seismology: Theory and methods: Vol. 1, W. N. Freeman & Co.
Alkhalifah, T., and Tsvankin, I., 1995, Velocity analysis for transversely isotropic media: Geophysics, **60**, 1550–1566.
Anderson, J., and Tsvankin, I., 1994, Dip-moveout processing by Fourier transform in anisotropic media: 64th Ann. Internat. Mtg., Soc. Expl. Geophys., Expanded Abstracts, 1213–1216.
Banik, N. C., 1984, Velocity anisotropy of shales and depth estimation in the North Sea Basin: Geophysics, **49**, 1411–1419.
——— 1987, An effective parameter in transversely isotropic media: Geophysics, **52**, 1654–1664.
Ben-Menahem, A., 1990, *SH*-waves from point sources in anisotropic inhomogeneous media: Geophysics, **55**, 488–491.
Ben-Menahem, A., Gibson Jr., R. L., and Sena, A. G., 1991, Green's tensor and radiation patterns of point sources in general anisotropic inhomogeneous elastic media: Geophys. J. Int., **107**, 297–308.
Berryman, J. G., 1979, Long-wave elastic anisotropy in transversely isotropic media: Geophysics, **44**, 896–917.
Carrion, P., Costa, J., Ferrer Pinheiro, J. E., and Schoenberg, M., 1992, Cross-borehole tomography in anisotropic media: Geophysics, **57**, 1194–1198.

Dellinger, J., and Muir, F., 1993, Dix revisited: A formalism for rays in layered media: Can. J. of Expl. Geophys., **29**, 93–97.
Dix, C. H., 1955, Seismic velocities from surface measurements: Geophysics, **20**, 68–86.
Hake, H., Helbig, K., and Mesdag, C. S., 1984, Three-term Taylor series for $t^2 - x^2$ curves over layered transversely isotropic ground: Geophys. Prosp., **32**, 828–850.
Gajewski, D., 1993, Radiation from point sources in general anisotropic media: Geophys. J. Int., **113**, 299–317.
Helbig, K., and Schoenberg, M., 1987, Anomalous polarization of elastic waves in transversely isotropic media: J. Acoust. Soc. Am., **81**, No. 5, 1235–1245.
Kim, K. Y., Wrolstad, K. H., and Aminzadeh, F., 1993, Effects of transverse isotropy on *P*-wave AVO for gas sands: Geophysics, **58**, 883–888.
Larner, K., 1993, Dip-moveout error in transversely isotropic media with linear velocity variation in depth: Geophysics, **58**, 1442–1453.
Levin, F. K., 1971, Apparent velocity from dipping interface reflections: Geophysics, **36**, 510–516.
——— 1990, Reflection from a dipping plane—Transversely isotropic solid: Geophysics, **55**, 851–855.
Musgrave, M. J. P., 1970, Crystal acoustics: Holden Day, San Francisco.
Rommel, B. E., 1994, Approximate polarization of plane waves in a medium having weak transverse isotropy: Geophysics, **59**, 1605–1612.
Rüger, A., 1995, *P*-wave reflections and azimuthal dependence of AVO in transversely isotropic media: Center for Wave Phenomena Res. Rep. CWP-171.
Sams, M. S., Worthington, M. H., and Khanshir, M. S., 1993, A comparison of laboratory and field measurements of *P*-wave anisotropy: Geophys. Prosp. **41**, 189–206.
Sayers, C. M., 1994, The elastic anisotropy of shales: J. Geophys. Res., **99**, No. B1, 767–774.
Taner, M. T., and Koehler, F., 1969, Velocity spectra—digital computer derivation and applications of velocity functions: Geophysics, **34**, 859–881.
Thomsen, L., 1986, Weak elastic anisotropy: Geophysics, **51**, 1954–1966.
——— 1993, Weak anisotropic reflections: Offset dependent reflectivity, Castagna and Backus, Eds.: Soc. Expl. Geophys., 103–114.
Tsvankin, I., 1995a, Normal moveout from dipping reflectors in anisotropic media: Geophysics, **60**, 268–284.
——— 1995b, Body-wave radiation patterns and AVO in transversely isotropic media: Geophysics, **60**, 1409–1425.
Tsvankin, I., and Chesnokov, E., 1990a, Synthesis of body-wave seismograms from point sources in anisotropic media: J. Geophys. Res., **95**(B7), 11 317–11 331.
——— 1990b, Synthetic waveforms and polarizations at the free surface of an anisotropic half-space: Geophys. J. Int., **101**, 497–505.
Tsvankin, I., and Thomsen, L., 1994, Nonhyperbolic reflection moveout in anisotropic media: Geophysics, **59**, 1290–1304.
——— 1995, Inversion of reflection traveltimes for transverse isotropy: Geophysics, **60**, 1095–1107.
White, J. E., 1983, Underground sound: Application of sound waves: Elsevier Sci. Publ.
Winterstein, D. F., 1986, Anisotropy effects in *P*-wave and *S*-wave stacking velocities contain information on lithology: Geophysics, **51**, 661–672.
Wright, J., 1987, The effects of transverse isotropy on reflection amplitude versus offset: Geophysics, **52**, 564–567.